

# Very High Energy Gamma Rays and Origin of Galactic Cosmic Rays

F.A. Aharanion

*MPI-K, Saupfercheckweg 1, 69117 Heidelberg, Germany*

I discuss the crucial role of TeV gamma-ray observations for localization/identification of accelerators of galactic cosmic rays, and argue that the recent morphological and spectrometric studies of a number of galactic TeV sources, in particular shell-type SNRs, with the HESS array of atmospheric Cherenkov Telescopes, is an event of extraordinary importance for the solution of the century-old problem of origin of galactic cosmic rays.

## 1. INTRODUCTION

It is believed that gamma-ray astronomy should play a crucial role in solving the problem of origin of galactic cosmic rays (CRs). The realization of this seminal prediction recognized by pioneers of the field in the 1950's and 1960's (see e.g. Refs [1, 2]) is still considered as one of the major goals of  $\gamma$ -ray astronomy. The basic idea is simple and concerns both the acceleration and propagation aspects of CRs. Namely, while the localized  $\gamma$ -ray sources exhibit the sites of production/acceleration of CRs, the angular and spectral distributions of the diffuse galactic  $\gamma$ -ray emission provide unique information about the character of propagation of relativistic particles in galactic magnetic fields. The prime objective of this activity is the decisive test of the hypothesis that supernova remnants (SNRs) are responsible for the bulk of the observed CR flux up to  $10^{15}$  eV.

Since the discovery of CRs by Victor Hess in 1912, the origin of this radiation has remained a mystery. Despite the plentiful experimental material accumulated over the recent decades and extensive theoretical efforts, the physicists and astronomers do not have a clear concept which could explain all features of non-thermal particles detected from sub-relativistic energies to  $10^{20}$  eV.

The energy spectrum of the hadronic component of CRs has two distinct features - the so-called *knee* and *ankle* around  $10^{15}$  eV and  $10^{18}$  eV, respectively (see Fig.1). It is believed that all particles below the *knee* are of galactic origin, and that the Extremely High Energy Cosmic Rays above the *ankle* are produced outside the Galactic Disk (see e.g. Refs [3, 4] - in powerful extragalactic objects like Active Galactic Nuclei, Radiogalaxies and Clusters of Galaxies, or during solitary events like Gamma Ray Bursts. It is likely that the contributions of these two components become comparable somewhere between the *knee* and *ankle*.

The acceleration, accumulation and effective mixture of nonthermal charged particles, through their convection and diffusion in galactic magnetic fields, produce the so-called "sea" of galactic CRs. The average density of CRs throughout the Galactic Disk is determined by operation of all galactic sources over

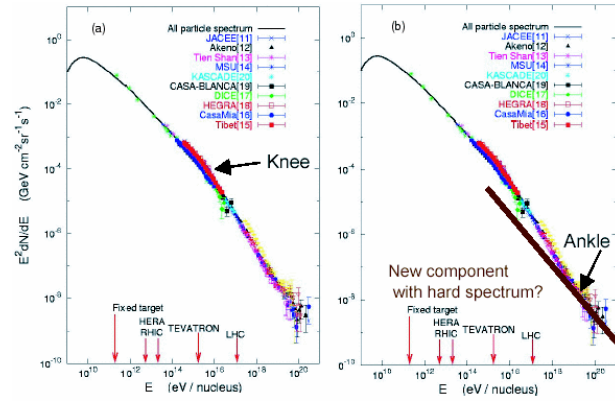


Figure 1: The energy spectrum of Cosmic Rays with indication of two features - the so-called "knee" (steepening of the spectrum above  $10^{15}$  eV) and "ankle" (hardening of the spectrum above  $10^{18}$  eV) [3].

a relatively long time period, comparable with the CR confinement time in the Galaxy of  $\sim 10^7$  yr (see e.g. Refs. [5]). If the level of the "sea" of CRs is not significantly different from the directly measured (local) CR flux, one can assume that the average energy density of CRs in the Galactic Disk should be around  $1 \text{ eV/cm}^3$ . Because of the relatively steep energy spectrum, more than 90 percent of this density is contributed by particles with energy  $\leq 100 \text{ GeV}$ .

The CR production rate in the Galaxy can be estimated solely on the basis of CR measurements, namely from the total flux and the secondary-to-primary ratio of CRs which contains information about the confinement time of CRs in the Galaxy. Remarkably, such an estimate is rather insensitive to the details characterizing the confinement region (density, volume, etc.). In particular, both the disk and halo CR confinement models give similar CR production rates [5]. The conservative estimates of the production rate of galactic CRs vary within  $(0.3 - 1) \times 10^{41} \text{ erg/s}$ .

This estimate of the CR production rate is based on the belief that charged particles during their propagation in the interstellar magnetic fields are well mixed, therefore the density of cosmic rays measured locally in the Solar neighborhood correctly reflects the level of the "sea" of CRs,  $w_{\text{CR}} = 1 \text{ eV/cm}^3$ . Although it is possible that a non-negligible fraction of the di-

rectly detected CR flux has *local* origin [6, 7], being contributed by handful nearby objects<sup>1</sup>, the EGRET measurements of the diffuse gamma-ray emission of the interstellar medium [8] show that the average CR density of relatively low energy ( $E \leq 100$  GeV) CRs in the Galactic Disk should be quite close to the locally measured CR density. Remarkably, the energy density of the "sea" of CRs of  $1\text{ eV/cm}^3$  is comparable with the pressure of galactic magnetic fields, as well as with the turbulent and thermal pressure of the interstellar gas. This implies that galactic cosmic rays play an important role in the dynamical balance of our Galaxy, and perhaps have also a non-negligible impact on *interstellar chemistry* through the heating and ionization of the interstellar medium (see e.g. Ref. [12]).

## 2. THE COMMON BELIEF

It is widely believed that Supernova Remnants (SNRs) constitute the major source population in our Galaxy responsible for the observed CRs. The main *phenomenological* argument, formulated by the pioneers of the field, is based on the fact that the power to maintain the galactic population of CRs is estimated to be  $\approx 10$  per cent of the total mechanical energy released by Sane explosions in our Galaxy. It is remarkable that as early as 1933 W. Baade and F. Zwicky realized the possible association of cosmic rays with supernovae, based on the comparable energies characterizing these two phenomena. This is, of course, a strong but not yet decisive point, given that other potential source populations like pulsars, X-ray binaries (microquasars), young stars with powerful mechanical winds also meet, at least formally, this energy requirement.

The second key argument in favor of SNRs as sources of galactic CRs has a theoretical background, namely it relies on the theory of diffusive shock acceleration (DSA) applied to young SNRs (see, for a recent review Ref. [13]). Over the last 20 years the basic properties of this model have been comprehensively studied and cross-checked using different computational approaches. In particular, it has been realized [14–16] that in effective accelerators the shocks are modified by the pressure of accelerated particles, and that this nonlinear effect should have a strong impact on the formation of the energy distribution of accelerated particles. On the other hand, since the ac-

celeration efficiency of CR accelerators, i.e. the fraction of mechanical energy transferred to non-thermal particles, should be very high, in the case of SNRs - 10 percent or more (in order to explain the production rate of galactic CRs), the theory of the nonlinear shock acceleration seems to be a key element in the SNR paradigm of galactic CRs.

DSA allows conclusive observational predictions. The distinct feature of this model is the very hard, power-law type (although not precisely power-law) energy distribution of particles with differential spectral index  $\alpha$  close to 2.

## 3. PROBING THE CONTENT OF COSMIC RAYS IN SUPERNOVA REMNANTS

The high acceleration efficiency, coupled with hard energy spectra of protons extending well beyond 10 TeV, should lead to VHE  $\gamma$ -ray fluxes of hadronic origin. Thus, the best way to check the hypothesis is to search for TeV  $\gamma$ -ray signals of  $\pi^0$ -decay origin from young shell-type SNRs [17]. TeV  $\gamma$ -rays have indeed been reported from three famous SNRs - SN 1006 [18], Cas A [19] RX J1713.7-3946 [20]. These are objects with nonthermal X-radiation of putative synchrotron origin radiated by  $\gg 10$  TeV electrons. Since the same electrons can also radiate TeV gamma-rays through inverse Compton (IC) scattering, we deal with two competing emission processes responsible for TeV radiation. It should be noted, however, that the leptonic origin of TeV gamma-ray emission from these SNRs was and remains the favored model of both the gamma-ray and X-ray communities. Moreover, the early observations of SNRs by the Whipple collaboration [21] were interpreted by many experts as a failure of SNRs in general, and DSA in particular, to be responsible for the production of galactic CRs. However, given the limited sensitivity of current detectors, as well as large uncertainties in several key model parameters, these conclusions in many cases are not well justified and, in fact, are misleading. Driven by an ultimate desire for dramatic revisions of the current concepts, the claims about the difficulties associated with gamma-ray observations of SNRs were premature and, to a large extent, exaggerated. A more rational conclusion from these observations was that only the stereoscopic IACT arrays with significantly improved sensitivity, and capability for adequate morphological and spectroscopic studies [22] could be able to probe the SNR visibility in  $\pi^0$ -decay  $\gamma$ -rays and thus to provide a decisive test for the SNR origin of galactic CRs.

---

<sup>1</sup>This statement is certainly true for at least very high energy CR electrons. Because of severe radiative losses, the source(s) of the observed TeV electrons cannot be located well beyond a few 100 pc [9], and therefore the sheer fact of extension of the observed electron spectrum to TeV energies is an unambiguous indicator of existence of a nearby cosmic *TeVatron*(s) [10, 11].

## 4. HESS - a powerful tool for probing shell-type SNRs in TeV gamma-rays

The success of ground-based gamma-ray astronomy (see e.g. Refs [23–26]) not only led to important astrophysical discoveries, but also elucidated the most effective and reliable detection techniques. Among the variety of competing designs, the *concept of stereoscopic arrays* consisting of 10m diameter or larger aperture telescopes was identified as the most convincing approach that can facilitate strong improvements in performance at an affordable cost, and, at the same time promises a fast scientific return [23].

The first representative of this class of IACT arrays dubbed HESS (High Energy Stereoscopic System) was completed in December 2003. The array consists of four 13m diameter optical dishes [27] spaced at the corners of a square of side 120 m, each equipped with a 960-pixel PMT camera with a field of view (FoV)  $\approx 5^\circ$  [28]. HESS operates in an effective energy range from 100 GeV to 30 TeV, with an angular resolution of a few arcminutes, energy resolution around 15 per cent, and a flux sensitivity of about 10 mCrab flux with a significance of  $5\sigma$  in 25 h of observations of a point like source [29], i.e. for sources with angular size less than the point spread function of the instrument,  $\delta\psi \simeq 0.1^\circ$ ). For an extended source with  $\theta \gg \delta\psi$ , the minimum detectable flux is increases approximately by a factor of  $\theta/\delta\psi$ .

Located in the Southern Hemisphere (Khomash Highland of Namibia), this  $5^\circ$  FoV stereoscopic array is currently the most sensitive instrument in the world to conduct morphological and spectrometric studies of extended galactic sources in TeV gamma-rays. The unique potential of HESS has been convincingly demonstrated by the discovery and study of a number of TeV sources representing several galactic and extragalactic source populations. The results on the spatial and energy distributions of TeV  $\gamma$ -rays of two young SNRs - RX J1713.7-3946 [30] and RX J0852.0-4622 (Vela Junior) [31], are of extraordinary importance, in particular in the context of origin of galactic cosmic rays.

### 4.1. RX J1713.7-3946

Discovered in X-rays during the ROSAT All-Sky Survey [32], this object later was extensively studied by the ASCA [33–35], Chandra [36], and XMM [37, 38] X-ray satellites. RX J1713.7-3946 was reported as a source of TeV emission by the CANGAROO collaboration [20, 39]. The HESS observations performed with two telescopes in 2003 confirmed this result, and, more importantly, provided a  $\gamma$ -ray image of this SNR on arcminute scales [40]. In 2004 the source was observed again, but this time with the full four-telescope system. The TeV image of the source based on  $\approx 40$  h

data sample [41] is shown in Fig.2. The signal from the entire remnant stands out from the residual charged CR background with a statistical significance of more than 40 standard deviations. The overall (asymmetric and thick) shell structure is clearly visible and correlates [40, 41] with the X-ray images detected with *ASCA* [34, 35] and *XMM-Newton* [37, 38], as well as with CO observations of a dense molecular gas complex located on the west side of the remnant [42].

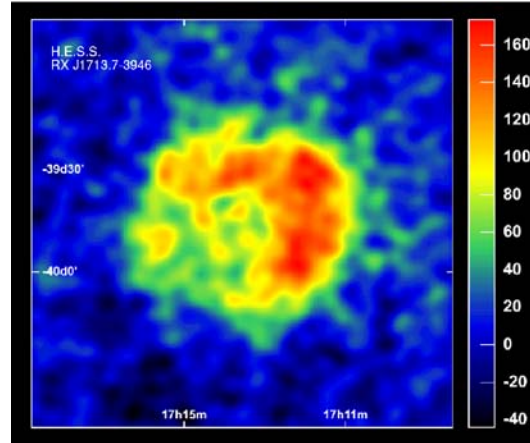


Figure 2: The gamma-ray image of RX J1713.7-3946 obtained with the 4-telescope array of HESS in 2004 [41]. The linear colour scale is in units of excess counts.

The energy spectrum of the entire remnant based on the 2003 data is shown in Fig.3. The experimental points in the energy interval 1-10 TeV can be described by a power-law with a photon index  $\Gamma = 2.19 \pm 0.09_{\text{stat}} \pm 0.15_{\text{syst}}$ . Although there is no indication for a spectral break, but a reasonable fit of data by a "power-law with exponential cutoff" (e.g. with  $\Gamma = 1.5$  and  $E_{\text{cut}} = 4$  TeV) cannot be excluded. The new HESS data obtained in 2004 allow significant extension of the energy spectrum towards 100 GeV and above 10 TeV, which hopefully will provide definite conclusions concerning the spectral features of this source.

The interaction of RX J1713.7-3946 with a nearby cloud discovered in CO observations by the *NANTEN* telescope [42] allows an estimate of the distance to the supernova remnant of about 1 kpc and, correspondingly, the age between 1 to 3 thousand years. If so, it is likely that RX J1713.7-3946 is a result of the supernova explosion which was registered in 393 A.D. as a guest star in the Chinese historical records [43]. Therefore RX J1713.7-3946 formally can be treated as a representative of young galactic SNRs like SN 1006, Vela Junior, Tycho, Kepler, Cas A.

However, RX J1713.7-3946 is, in fact, a unique object with very unusual characteristics. First of all this concerns the X-ray emission which does not contain a measurable thermal component. This could be an indication that the supernova explosion occurred in-

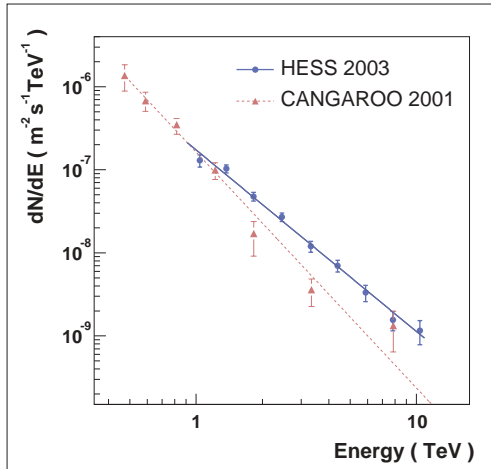


Figure 3: The  $\gamma$ -ray spectrum of RX J1713.7-3946 reported by the HESS collaboration [40] and by the CANGAROO collaboration [39]. Note that while the HESS points are for the whole remnant, the CANGAROO points correspond to the northwestern (NW) part of the remnant. This implies a factor of 3 difference in reported fluxes at 1 TeV.

side the wind-blown bubble with very low gas density [34]. A different explanation for the lack of thermal X-ray emission is also possible, namely assuming a very high density environment; because of the fast radiative cooling, the dense ambient gas cannot be heated to sufficiently high temperatures to emit thermal X-rays.

The observed spatial correlation of the X-ray emission with the CO map of the brightest west portion of the remnant [37, 38, 42] could be interpreted as an argument in favor of the production of nonthermal X-rays in the dense gas regions. On the other hand, the X-ray emission with hardest power-law spectrum, as observed by *XMM-Newton* from the South-East part of the remnant [37], shows that we deal with a very complex system, and many issues, even the commonly accepted model of synchrotron X-ray emission, should be subject of detailed examination and further studies.

Meanwhile, these questions are tightly related to the observed TeV  $\gamma$ -ray emission, and therefore their solution would be crucial also for understanding of the origin of TeV gamma-rays. Indeed, the first scenario, which assumes very low plasma density ( $n \leq 10^{-2} \text{ cm}^{-3}$ ), excludes any hope for detection of TeV gamma-rays of hadronic origin. The second scenario, which assumes very high density environment, disfavors the Inverse Compton (IC) origin of the observed IC gamma-rays, unless one assumes a very clumpy environment with "voids" (regions of low-density gas and low-magnetic field) where the TeV electrons spend significantly more time than in dense clouds. The real picture could be, in fact, more com-

plex. Clearly, significant efforts in modeling of particle acceleration, propagation and radiation processes based on high quality multiwavelength observations of several SNRs are needed before any conclusion concerning the origin of nonthermal radiation, and correspondingly the acceleration rates and spectra of electrons and protons in these objects.

In this regard it is difficult to underestimate the importance of the recent reports of detection of TeV  $\gamma$ -ray emission from another young supernova remnant - RX J0852.0-4622 (or Vela Junior) by the CANGAROO [44] and HESS [45] collaborations.

## 4.2. Vela Junior

Vela Junior was discovered using the data of the ROSAT All-Sky Survey [46]. The distance and the age of the source are estimated by different authors between 200 pc [47] and 1 kpc [48] and between several hundred to several thousand years, respectively.

The X-ray image shows a quasi-regular  $2^\circ$  diameter ring-like structure with enhanced emission along the northern, western, and southeastern limbs. The source displays also X-ray emission from the interior - a faint X-ray point-like source (a neutron star?) surrounded by a diffuse nonthermal component (a synchrotron nebula?).

The X-ray flux is dominated, like in SNRs RX J1713.7-3946 and SN 1006, by a nonthermal component. The radio and X-ray fluxes of Vela Junior and SN 1006 are rather similar: several times  $10^{-13} \text{ erg/cm}^2\text{s}$  around 1 GHz and  $\sim 10^{-10} \text{ erg/cm}^2\text{s}$  in the 1-10 keV band, correspondingly. The relation of radio and X-ray fluxes is quite different in the case of RX J1713.7-3946. While the radio flux of this SNR is an order of magnitude less than the radio flux of Vela Junior, its X-ray flux exceeds by a factor of 5 the X-ray flux of Vela Junior. Despite this difference, the faint synchrotron radio flux is a common feature of these three objects. Other young SNRs, in particular Cas A, Tycho and Kepler, the X-ray emission of which is dominated by thermal components, are much stronger radio sources.

The similarity between RX J1713.7-3946 and Vela Junior is supported also by the strong extended TeV emission of both objects spatially correlated with X-rays. The HESS image of Vela Junior in TeV  $\gamma$ -rays is shown Fig.4. The energy spectrum in the energy range between 500 GeV and 15 TeV is described by a power-law,  $dN/dE = \Phi(E/1 \text{ TeV})^{-\Gamma}$  with  $\Gamma = 2.1 \pm 0.1_{\text{stat}} \pm 0.1_{\text{syst}}$  and  $\Phi = (2.1 \pm 0.2_{\text{stat}} \pm 0.6_{\text{syst}}) \times 10^{-11} \text{ cm}^{-2}\text{s}^{-1}\text{TeV}^{-1}$ . Compared to RX J1713.7-3946, the total flux of Vela Junior is somewhat higher, and the spectrum seems to be slightly harder.

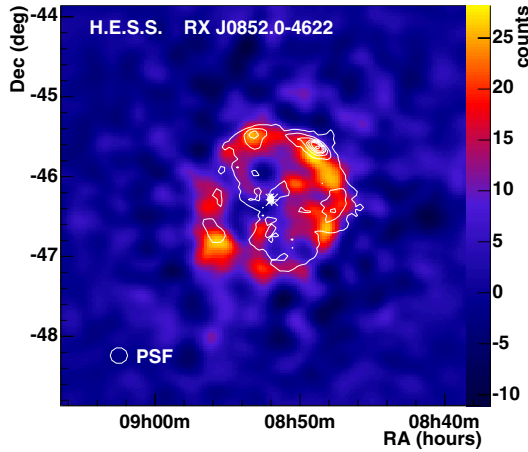


Figure 4: The HESS image of the SNR Vela Junior obtained with the 4-telescope HESS array [45]. The excess of  $660 \pm 60$  events from the whole remnant with a  $12\sigma$  statistical significance is obtained in 4.5 h observation time in 2004. The image is smoothed with a Gaussian of standard deviation of 6 arcmin. The point spread function of HESS is shown by a circle. The superimposed ASCA contour lines [48] show spatial correlation between X-rays and TeV  $\gamma$ -rays. The position of the neutron star candidate AXJ0851.9-4617.4 is marked with an asterisk.

### 4.3. SN 1006

The claim of detection of TeV  $\gamma$ -ray emission of this young shell-type supernova remnant by the CANGAROO collaboration [49] initiated a number of phenomenological and theoretical studies to explain the high energy  $\gamma$ -ray emission within the leptonic (e.g. Refs.[50–53]) or hadronic (e.g. Refs. [52, 54]) models.

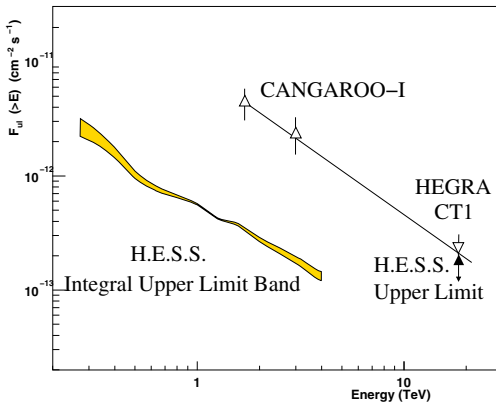


Figure 5: Comparison of observations of SN1006 reported by HESS [55] and CANGAROO [49] from the same (NW) part of the shell. The HESS upper limit (99.9% c.l.) band is derived assuming a photon index from  $\Gamma=2$  to 3.

The HESS observations of SN 1006 have been carried in 2003 and 2004 [55]. No evidence for TeV

gamma ray emission from any compact or extended region associated with the remnant was obtained. The upper limit on the TeV flux (see Fig. 5) is below, by an order of magnitude, the flux reported by the CANGAROO group. This upper limit constrains (1) the total energy in  $\geq 1$  TeV protons in the remnant,  $W_p \leq 10^{50} (d/2 \text{ kpc})^2 (n/0.1 \text{ cm}^{-3})^{-1}$  erg ( $n$  is the number density of the gas in the confinement region of protons) within the framework of hadronic models, and (2) the strength of the post-shock magnetic field  $B \geq 25 \mu\text{G}$  within the framework of leptonic (IC) models 5.

## 5. THE CASE OF CASSIOPEIA A

The shell type supernova remnant Cas A is the brightest radio source in our Galaxy. The synchrotron radiation of Cas A continues to submillimeter wavelengths, and perhaps even further to the infrared and hard X-rays. The magnetic field in this young SNR is very high. By comparing the bremsstrahlung flux of radio emitting electrons with the gamma-ray flux upper limit  $J(> 100 \text{ MeV}) \leq 1.1 \times 10^{-6} \text{ ph/cm}^2 \text{s}$  set by the COS B and EGRET high energy gamma-ray detectors, one can derive a robust low limit [56, 57] for the magnetic field in Cas A at the level of  $B_0 \approx 100 \mu\text{G}$ . Such a constraint on the magnetic field is possible because of the high radio flux of Cas A and effective production of high energy  $\gamma$ -rays via electron bremsstrahlung. Actually this is a quite unusual situation compared with other shell type isolated SNRs for which bremsstrahlung is generally ineffective  $\gamma$ -ray production mechanism. The reason is twofold: a very large amount of electrons with energy extending to at least 10 GeV (the electrons which produce synchrotron radiation at mm wavelengths), and large gas density,  $n \geq 10 \text{ cm}^{-3}$ . There is little doubt that GLAST should detect this radiation component at MeV/GeV energies, and thus provide an unambiguous probe of the magnetic field in Cas A.

Cas A is the result of the youngest supernova event in our Galaxy that took place around 1680. The source is bright in X-rays, a noticeable fraction of which may have nonthermal (synchrotron) origin [58]. The same multi-TeV electrons responsible for synchrotron X-rays contribute to the TeV  $\gamma$ -ray emission through the inverse Compton scattering. However, because of the strong magnetic field, the efficiency of inverse Compton channel in this object seems to be quite low.

The “brute-force” observation strategy applied by the HEGRA collaboration to this prominent objects, was eventually rewarded by detection of a tiny flux ( $5.8 \pm 1.2_{\text{stat}} \pm 1.2_{\text{syst}} \times 10^{-13} \text{ ph/cm}^2 \text{s}$  above 1 TeV [19]). More than 200 hours of data accumulated during 3 years from 1997 to 1999, revealed a positive signal with statistical significance exceeding  $5\sigma$ .

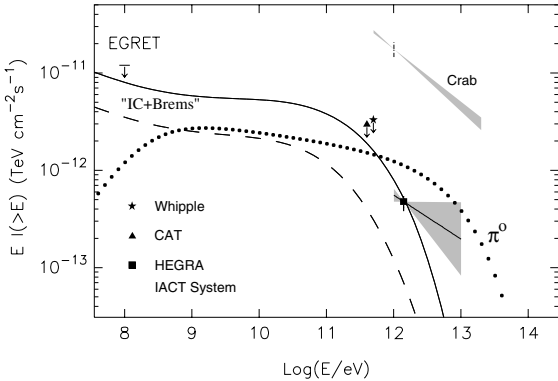


Figure 6: Gamma-rays from Cas A. The shaded area shows the  $1\sigma$  error range for the fluxes measured by the HEGRA CT-system [19]. Also indicated are the flux upper limits set by EGRET, Whipple and CAT telescopes. Model predictions are presented by solid, dashed and dotted curves. The dotted curve represents the fluxes for  $\pi^0$ -decay decay  $\gamma$ -rays calculated for relativistic protons with power-law index  $\Gamma = 2.15$  (identical to the spectral index of radio emitting electrons), exponential cutoff at  $E_0 = 200$  TeV and total energy  $2 \times 10^{49}$  erg. The density in the shell is assumed  $n = 15 \text{ cm}^{-3}$ . The solid and dashed lines correspond to the  $\gamma$ -ray fluxes produced by electrons calculated in the framework of a 3-zone model for 2 set of basic parameters discussed in Ref. [57].

The interpretation of this signal in terms of IC  $\gamma$ -rays seems unlikely, unless one assume multi-zone structures containing regions with low B-field “voids” [57]. On the other hand, because of the low TeV  $\gamma$ -ray flux and high average density of the nebular gas, a little effort is needed to explain the TeV radiation by interactions of accelerated protons [57, 59]. This interpretation requires  $\approx 10^{49}$  erg total energy in accelerated protons (see Fig. 6) which exceeds the energy in relativistic electrons only by a factor of  $\leq 10$ .

A crucial information about the  $\gamma$ -ray production mechanism is contained in the energy spectrum. The inverse Compton model predicts quite steep TeV  $\gamma$ -ray spectrum with a photon index  $\Gamma \sim 3$ . Therefore the detection of a hard  $\gamma$ -ray spectrum would be a strong argument in favor of the hadronic origin of the TeV emission. The TeV flux of Cas A is rather weak, therefore accurate measurements of the energy spectrum can be performed only with new generation IACT arrays, like MAGIC and VERITAS, located in the Northern Hemisphere.

## 6. Hadronic versus leptonic gamma-rays

The key objective of TeV observations of the shell-type SNRs, at least in the context of origin of galactic CRs, is the detection/identification of the hadronic component of  $\gamma$ -ray emission related to the shock-

accelerated protons and nuclei. In this regard, the understanding of the origin of TeV  $\gamma$ -ray images detected from RX J1713.7-3946 and Vela Junior is of great importance, and may lead to the first strong observational evidence of acceleration of multi-TeV protons in SNRs. For such a dramatic conclusion we need to show that the TeV signal *cannot* be related to relativistic electron. Since we have only two real alternatives (IC or  $\pi^0$ -decay gamma-rays), the demonstration of the failure of the IC mechanism to explain the TeV data would be interpreted as a proof of the hadronic origin of TeV radiation. Therefore, comprehensive theoretical and phenomenological studies of both leptonic and hadronic models of  $\gamma$ -ray production in SNRs are equally important for the solution of the origin of Galactic Cosmic Rays.

For a standard “power-law with exponential cutoff” energy distribution of protons,

$$Q(E) \propto E^{-\alpha} \exp(-E/E_0), \quad (1)$$

the flux of  $\gamma$ -rays produced in the interactions of CR protons with the ambient gas is basically determined by the scaling parameter

$$A = \left( \frac{W_{\text{CR}}}{10^{50} \text{ erg}} \right) \left( \frac{d}{1 \text{ kpc}} \right)^{-2} \left( \frac{n}{1 \text{ cm}^{-3}} \right), \quad (2)$$

where  $W_{\text{CR}}$  is the total energy in accelerated protons,  $n$  is the ambient gas density, and  $d$  is the distance to the source. The  $\gamma$ -ray spectrum at high energies repeats the spectral shape of parent protons – a power-law with approximately the same power-law index  $\Gamma \approx \alpha$ , and a cutoff at  $E \sim 0.1E_0$ . For the given energy density of accelerated protons, the integral flux of  $\gamma$ -rays above 300 MeV is almost independent of the proton spectral index,

$$J_\gamma (\geq 300 \text{ MeV}) \approx 3 \cdot 10^{-8} A \text{ cm}^{-2} \text{s}^{-1}. \quad (3)$$

At energies  $1 \text{ GeV} \leq E \leq 0.1E_0$ , and for the standard chemical composition of CRs and the ambient gas,

$$J_\gamma (\geq E) = 10^{-11} E_{\text{TeV}}^{-\alpha+1} A f_\alpha \text{ cm}^{-2} \text{s}^{-1}, \quad (4)$$

where  $f_\alpha \approx 1$  and 0.2 for the the proton spectral indices  $\alpha = 2$  and 2.3, respectively. The integral fluxes of  $\pi^0$ -decay  $\gamma$ -rays from a  $10^3$  yr old SNR for the scaling parameter  $A = 1$ , and proton spectrum with  $\alpha = 2$  and  $E_0 = 100$  TeV, are shown in Fig. 7.

When deriving information about the accelerated protons one has to take into account a possible non-negligible “contamination” caused by directly accelerated electrons that upscatter photons of the 2.7 K CMBR (the dominant target photon field in most of SNRs) to  $\gamma$ -ray energies. The multi-TeV electrons responsible for TeV  $\gamma$ -rays produce also synchrotron UV/X radiation. The typical energies of the IC and synchrotron photons produced by the same electron are related by

$$E_\gamma \simeq 2(\varepsilon_x / 0.1 \text{ keV})(B / 10 \mu\text{G})^{-1} \text{ TeV}. \quad (5)$$

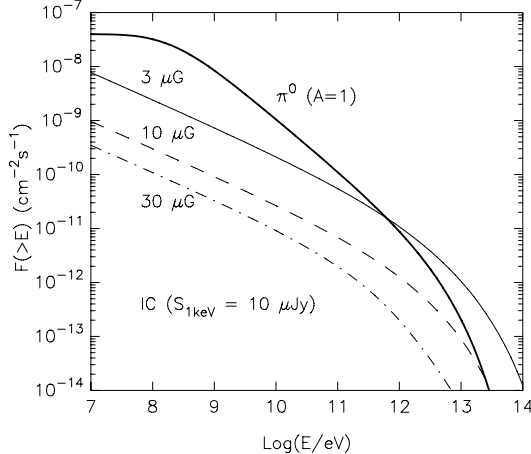


Figure 7: Fluxes of  $\pi^0$ -decay (heavy solid line) and IC (thin lines)  $\gamma$ -rays from a  $10^3$  year old SNR. The  $\pi^0$  decay  $\gamma$ -rays are calculated for the scaling parameter  $A = 1$ . The IC  $\gamma$ -ray fluxes are calculated for 3 different values of the magnetic field:  $B = 3$  (solid curve), 10 (dashed curve), and  $30 \mu\text{G}$  (dot-dashed curve), assuming that the electrons produce the same flux of synchrotron X-radiation  $S_\nu = 10 \mu\text{Jy}$  at 1 keV. For both protons and electrons the same acceleration spectrum given by Eq.(1) is assumed with  $\alpha = 2$  and  $E_0 = 100 \text{ TeV}$ .

Note that this relation neglects the Klein-Nishina effect which however becomes important at energies  $E_\gamma \geq 10 \text{ TeV}$ . The ratio of the synchrotron and IC fluxes  $f_E \equiv E^2 F(E) = \nu S_\nu$  at energies given by Eq.(5) depends on the magnetic field:

$$\frac{f_{\text{IC}}(E_\gamma)}{f_{\text{sy}}(\varepsilon_x)} \simeq 0.1 (B/10 \mu\text{G})^{-2}. \quad (6)$$

For a flat X-ray spectrum with photon index  $\simeq 2$ , the energy flux  $f_X$  slightly depends on energy. Therefore  $f_X$  at a typical energy of 1 keV could serve as a good indicator of the level of the IC  $\gamma$ -ray flux at TeV energies, albeit for the field  $B \ll 100 \mu\text{G}$  the energy of synchrotron photons (produced by the same parent electrons) related directly to  $\sim 1 \text{ TeV}$   $\gamma$ -rays is in the UV/soft X-ray band.

The contribution of  $\pi^0$ -decay  $\gamma$ -rays dominates over the contribution of the IC component if

$$A \geq 0.1 (S_{1\text{keV}}/10 \mu\text{Jy}) (B/10 \mu\text{G})^{-2}, \quad (7)$$

where  $S_{1\text{keV}}$  is the flux of nonthermal synchrotron radiation at 1 keV normalized to  $10 \mu\text{Jy}$  (the corresponding energy flux  $f_X \approx 2.4 \times 10^{-11} \text{ erg/cm}^2\text{s}$ ).

In Fig. 7 the integral fluxes of  $\pi^0$ -decay and inverse Compton  $\gamma$ -rays from a SNR of age  $10^3$  yr are shown. The  $\pi^0$ -decay  $\gamma$ -ray flux corresponds to the scaling factor  $A = 1$ . The IC fluxes are calculated by normalizing the synchrotron X-ray flux to  $S_{1\text{keV}} = 10 \mu\text{Jy}$  for different values of ambient magnetic field. Note that for the normalizations used,

the results presented in Fig. 7 only slightly depend on the source age, unless it is larger than the synchrotron cooling time of multi-TeV electrons,  $t_{\text{synch}} \approx 1.2 \times 10^3 (B/10 \mu\text{G})^{-2} (E_e/100 \text{ TeV})^{-1} \text{ yr}$ .

## 7. The case of RX J1713.7-3946

In Fig. 8 the broad-band spectral energy distribution (SED) of RX J1713.7-3946 is shown, together with the SED of Vela Junior. While in the case of RX J1713.7-3946 the ratio of the energy flux of  $\gamma$ -rays at several TeV to the X-ray flux at 1 keV is about 0.1, for Vela Junior this ratio is close to 1. In accordance with Eq.(6) the interpretation of TeV fluxes within the one-zone Synchrotron-IC model requires quite low magnetic fields – about  $10 \mu\text{G}$  and  $3 \mu\text{G}$  for RX J1713.7-3946 and Vela Junior, respectively. The accurate time-dependent calculations within the one-zone model presented in Fig. 8 confirm these estimates for the magnetic field.

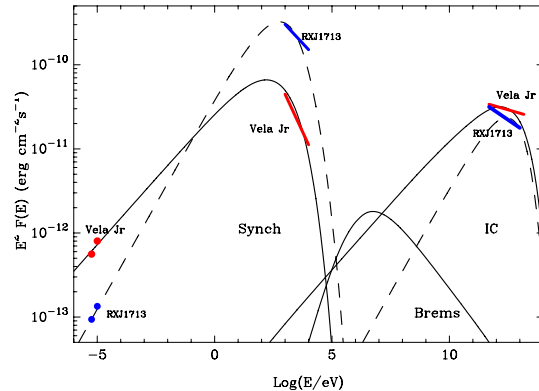


Figure 8: The integrated broad band SEDs of RX J1713.7-3946 and Vela Junior, and their interpretation within the framework of the one-zone leptonic model. The shown power-law presentations of gamma-ray fluxes are from the best fits to the HESS data. Three components of radiation - synchrotron, IC and bremsstrahlung - are shown. The calculations for RX J1713.7-3946 are performed for the following parameters: electrons are accelerated and injected continuously, over the last 1000 yr, into a region with magnetic field  $10 \mu\text{G}$  and gas density  $n = 0.1 \text{ cm}^{-3}$ . It is assumed that the electrons are injected with a rate  $L_e = 10^{37} (d/1\text{kpc})^2 \text{ erg/s}$  and energy spectrum given by Eq.(1) with  $\alpha = 2$  and  $E_0 = 50 \text{ TeV}$ . The model parameters used for calculations of the SED of Vela Junior are similar, except for  $\alpha = 2.37$ , and  $L_e = 8 \times 10^{38} (d/1\text{kpc})^2 \text{ erg/s}$ .

Generally, these are uncomfortably low values for the B-field in these SNRs. Indeed, for the given synchrotron X-ray spectra of these sources which are extended to 10 keV, the above condition of low magnetic field implies extension of the electron spectrum to  $E \simeq 250 (\varepsilon_0/1\text{keV})^{1/2} B_{\mu\text{G}}^{-1/2} \text{ TeV}$ , where

$\varepsilon_0$  is the cutoff energy in the spectrum of synchrotron X-rays,  $B_{\mu G} = B/1\mu G$  is the magnetic field in units of  $\mu G$ . On the other hand, the maximum (within the framework of standard DSA model) energy of electrons, assuming that the acceleration proceeds in the extreme Bohm diffusion limit, and neglecting the radiative losses of electrons, is estimated  $E \simeq 8(\tau_0/10^3 yr)(v/3000 km/s)^2 B_{\mu G}$  TeV ( $\tau_0$  is the age of the source and  $v$  is the shock speed). From these two conditions we may conclude that the magnetic field should exceed  $B_{\mu G} \simeq 10(\tau_0/10^3 yr)^{-2/3}(v/3000 km/s)^{-4/3}(\varepsilon_0/1 keV)^{1/3}$  in order to explain the cutoff energy in the X-ray spectrum  $\varepsilon_0 \geq 1$  keV.

Thus, while the IC interpretation of TeV  $\gamma$ -rays from RX J1713.7-3946 and Vela Junior requires B-fields around  $10 \approx \mu G$  and  $3\mu G$ , respectively, the spectra of synchrotron X-ray emission of both objects require, even under the most favorable conditions,  $B \geq 10 \mu G$ . This discrepancy can be solved if one assume that a more effective acceleration mechanism (compared to the "standard" parallel shock acceleration model; see Ref.[60]) operates in these objects. Also, significantly larger magnetic field in the accelerator could be allowed assuming that the electron acceleration and IC emission regions are separated. Even so, the total X-ray flux should be dominated by the radiation produced in the TeV  $\gamma$ -ray production region(s) which follows from the spatial correlation between the TeV and X-ray images of RX J1713.7-3946 [40]. This implies that the sites of particle acceleration should be quite compact. Fig.9 demonstrates that the two-zone model applied to the NW rim of RX J1713.7-3946 (assuming that electrons are accelerated in the thin filaments resolved by *Chandra*) allows relatively large magnetic field in filaments and, at the same time, quite high flux of TeV  $\gamma$ -rays in the plateau region [36]. Note that the predicted  $\gamma$ -ray flux is a factor of 2-3 below the flux detected by HESS from the same NW region. However, the IC  $\gamma$ -ray flux can be significantly increased assuming slightly faster escape of electrons from filaments. It should be noted also that although in the two-zone model the particle accelerators should appear as distinct sites because of their high surface brightness of the synchrotron X-radiation (seen in the forms of filaments and hot spots), the total X-ray flux from the plateau region is still significantly larger than from the filaments and hot spots.

Although the absolute  $\gamma$ -ray fluxes can be explained by the IC mechanism, at least within the two-zone model, the flat power-law  $\gamma$ -ray spectrum observed from RX J1713.7-3946 with power-law index  $\approx 2.2$  (in the interval 1-10 TeV) do not fully agree with the theoretical IC spectra. The reason is the following. The electrons do not suffer significant energy losses up to  $E \sim 100(B/10\mu G)^{-2}(\tau_0/1000 yr)^{-1}$  TeV, and therefore keep their hard (acceleration) spectrum

unchanged during the age of the source  $\sim 1000$  yr. Consequently, we should expect very hard IC  $\gamma$ -ray spectra below 10 TeV. On the other hand, one should require a cutoff or steepening of the electron spectrum around 100 TeV to fit the detected X-ray spectrum. This feature, coupled with the Klein-Nishina effect, leads to a break in the IC spectrum above several TeV. Thus we should expect a "bell-type" SED of  $\gamma$ -rays with a maximum between 1 and 10 TeV. Such a spectral shape *does not match* the power-law spectrum of TeV  $\gamma$ -rays observed from RX J1713.7-3946

Somewhat better IC fits to the HESS data are possible if we assume (i) a steeper acceleration spectrum, or (ii) significant non-radiative losses, e.g. due to the energy-dependent escape of electrons from the zone 2. The first possibility is demonstrated for Vela Junior in Fig. 8. The electron acceleration spectrum with  $\alpha \simeq 2.4$  fits well also the radio data. However such a spectrum requires very high injection power,  $L_e = 8 \times 10^{38}$  erg/s. Therefore, from the point of view of overall energetics, the steepening of the electron spectra due to escape losses, seems a more feasible option.

Unlike the IC models, the hadronic models of TeV radiation of SNRs are less restricted by the multi-wave observations at other wavelengths. Moreover, with a choice of two parameters characterizing the acceleration spectrum of protons, i.e. the power-law index  $\alpha$  and the cutoff energy  $E_0$ , it is possible to explain a rather broad range of  $\gamma$ -ray spectra. The main problem connected with the hadronic model is the low efficiency of conversion of energy of accelerated protons to TeV  $\gamma$ -rays. The characteristic time of radiative cooling of protons interacting with the ambient matter of density  $n$  through the  $\pi^0$ -channel is  $t_{pp \rightarrow \pi^0} \approx 1.5 \times 10^8(n/1 cm^{-3})^{-1}$  yr which is longer, by many orders of magnitude, than the most active epoch of acceleration of particles in a SNR to multi-TeV energies (typically, the first  $10^3$  yrs after the SN explosion). Nevertheless, such a slow radiative cooling of protons appears sufficient, as it follows from Eq.(4), to make SNRs visible in TeV  $\gamma$ -rays, if the parameter  $A \geq 0.1$ . Most likely, this is the case of RX J1713.7-3946 - a young ( $t \sim 10^3$  yr old), nearby ( $d \sim 1$  kpc) and powerful SNR exploded in a dense gas environment.

The flux and the energy spectrum of RX J1713.7-3946 can indeed be explained by interactions of protons with the ambient gas, through production and decay of secondary  $\pi^0$ -mesons. Since the spectra of RX J1713.7-3946 does not show spectral cutoff up to 10 TeV, one may conclude that the proton spectrum should continue without a break, up to 100 TeV.

For the reported integral flux and energy spectrum of TeV  $\gamma$ -rays from RX J1713.7-3946,  $J(\geq 1 \text{ TeV}) \simeq 1.5 \times 10^{-11} \text{ ph/cm}^2 \text{s}$  and  $\Gamma \simeq 2.1 - 2.3$ , Eqs.(2) and (4) give the following estimate of the re-

quired total energy in protons,  $W_{\text{CR}} \simeq (1.5 - 7.5) \times 10^{50} (d/1\text{kpc})^{-2} (n/1\text{cm}^{-3})$  erg. Given the recent estimates of the distances to this sources of about 1 kpc [42], and the theoretical conviction that approximately 10 percent of the mechanical energy of the SN explosion is converted into relativistic protons, the detected TeV fluxes can be explained for the average density of the ambient gas in the  $\gamma$ -ray production region of about several hydrogen atoms or molecules per  $1\text{cm}^3$ . This is a quite modest requirement which can be provided by the shock-compressed gas in the shell or by the surrounding dense gas environment.

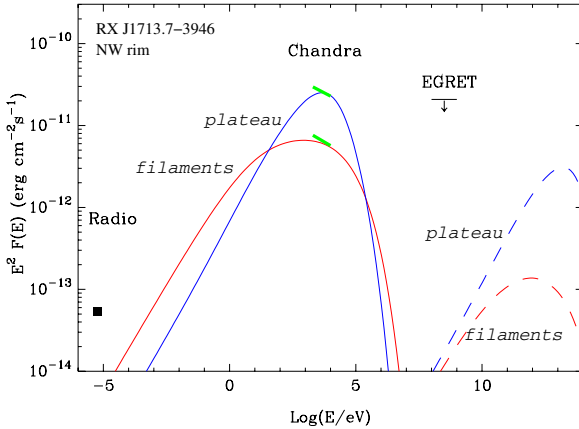


Figure 9: Multiwavelength synchrotron (solid lines) and IC (dashed lines) spectra of filaments and the "plateau" regions of the NW rim of RX J1713.7-3946 calculated within the *two-zone* model, under the assumption that the electron acceleration takes place in filaments. The following parameters have been used in calculations: age  $\tau_0 = 1000$  yr, the electron acceleration rate in filaments  $L_e = 4 \times 10^{36} (d/1\text{kpc})^2$  erg/s,  $\alpha = 1.95$ ,  $E_0 = 200$  TeV,  $B_{\text{fil}} = 20 \mu\text{G}$ ,  $B_{\text{plat}} = 6 \mu\text{G}$  the time of convection escape 500 yr. The details are described in Ref. [36].

The interpretation of the TeV gamma-ray emission reported by the CANGAROO group in terms of hadronic interactions [39] has been criticized with an objection that the canonical shock-acceleration spectrum of protons with power-law index  $\alpha = 2$  would result in violation of the EGRET upper limits at GeV energies [61, 62]. Formally, this objection stands also for the HESS results. However, this is not a sufficiently robust and convincing argument to dismiss the hadronic origin of the TeV signal [36]. A slightly harder proton spectrum, e.g. with spectral index,  $\alpha \leq 2$ , coupled with relatively small high energy cut-off energy,  $E \leq 100$  TeV, can easily avoid the conflict with the EGRET data, but yet explain satisfactorily the TeV flux and spectrum. Moreover, even for a proton spectrum steeper than  $\alpha = 2$ , it is possible to suppress the GeV  $\gamma$ -ray flux by invoking the effect of the energy-dependent propagation of protons when they travel from the accelerator (SNR shock) to the

target (nearby gas clouds) [63]. In particular, the lack of GeV  $\gamma$ -rays can be naturally explained by the confinement of low energy protons in the supernova shell.

In any case, it is clear that the standard DSA models cannot be applied for calculations of  $\gamma$ -ray emission from a SNR interacting with dense molecular clouds. In particular, in such systems one has to treat thoroughly the spectral features of particles *ahead of the shock*. Indeed, this component of relativistic protons is most relevant to the TeV  $\gamma$ -ray emission observed from RX J1713.7-3946, if  $\gamma$ -ray production occurs when the SNR shock approaches a dense gas region as discussed in Ref. [64]. In this paper several important features of particle acceleration, in particular the *nonlinearity* of the acceleration process (i.e. the modification of the flow by accelerated particles) and the position-dependent *low-energy cutoff* in the spectrum of accelerated particles ahead of the shock, have been included in calculations. Note that the low-energy cut-off is unavoidable in the upstream of the shock. This effect was ignored in the past, because in the shock acceleration models usually only the downstream solutions were considered (the downstream spectrum of particles is almost coordinate-independent). However, at the presence of a dense gas region upstream of the shock, the  $\gamma$ -ray production is dominated by p-p interactions in these regions, and therefore the low energy cutoff becomes an important factor. Finally, the energy-dependent escape of particles from the cloud is another important effect which leads to the high-energy break (steepening) in the proton, and, consequently, also in the secondary  $\gamma$ -ray spectrum.

The approach suggested in Ref. [64] is applicable also for the electronic component of accelerated particles; the electrons enter the cloud with a low-energy spectral cutoff as well. If so, the high gas density and the large magnetic field in the adjacent molecular clouds (typically  $\geq 25 \mu\text{G}$ ; see e.g. Ref. [65]), can naturally explain the spatial correlations of both X-ray and TeV  $\gamma$ -ray images with CO maps, as well as the very low radio flux of RX J1713.7-3946 [66]. Generally, molecular clouds have clumpy structure with inter-clump gas density exceeding  $10 \text{ cm}^{-3}$  (see e.g. Ref. [67]). This implies that approximately  $10^{49} - 10^{50}$  erg is required in accelerated protons to explain the observed TeV  $\gamma$ -ray flux.

The energy spectrum reported by the HESS collaboration based on the 2003 (2-telescope) data cover a relatively narrow energy band, from 1 TeV to 10 TeV. In this regard, the new measurements of the energy spectrum of RX J1713.7-3946 performed in 2004 with the full 4-telescope array, should allow an extension of the energy band towards 100 GeV and 30 TeV which hopefully could provide stronger evidence of association of the TeV  $\gamma$ -ray emission with the dense gas regions, and thus the hadronic origin of the parent particles.

Finally we note that if a significant fraction of the

TeV  $\gamma$ -ray signal of RX J1713.7-3946 is indeed of neutral pion origin, then the accompanying charged pions will produce a guaranteed neutrino flux above the sensitivity threshold of the future kilometer-scale high energy Neutrino Observatories [4].

## 8. Other TeV source populations

The detection of TeV  $\gamma$ -ray images of RX J1713.7-3946 and Vela Junior is a great success which clearly demonstrates that young shell-type SNRs are effective factories of multi-TeV particles. However, these results do not yet allow us to arrive at a more general conclusion, namely, that SNRs provide the bulk of the flux of galactic cosmic rays up to the knee around  $10^{15}$  eV. One cannot exclude that some other galactic source populations, e.g. pulsars and their ultra-relativistic winds, X-ray binaries, in particular micro-quasars, contribute comparably to the observed cosmic ray flux. The recent HESS discoveries of TeV  $\gamma$ -rays from the composite SNR G0.9+0.1 [68] (see Fig.10), pulsar wind nebula MSH 15-52 [69], and the binary pulsar PSR B1259-63 [70] show that there are indeed other classes of galactic *TeVatrons*.

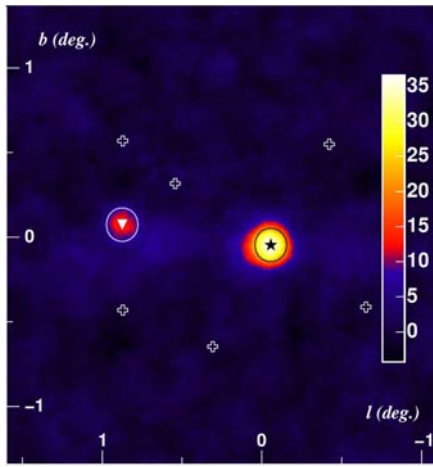


Figure 10: Gamma-ray point source significance map for the region around the Galactic Center. Two sources of TeV gamma-rays are clearly visible: the Galactic Center (HESS J1745-290) and a second source (HESS J1747-281) coincident with the composite supernova remnant G 0.9+0.1. The gamma-ray emission of G 0.9+0.1 appears to originate in the plerionic core of the remnant, rather than in the shell [68].

It should be noted in this regard that the  $\gamma$ -ray spectrum of the Crab Nebula - the strongest pulsar-wind nebula in our Galaxy - extends to  $\geq 50$  TeV [71] (see Fig. 11). Although it is widely believed that the pulsar winds are electron accelerators, one cannot exclude that a non-negligible fraction of the energy carried by the pulsar wind is released in the form of PeV nuclei [72-74].

Finally, the detection of TeV  $\gamma$ -rays from the direction of the Galactic Center by the CANGAROO, Whipple and HESS collaborations [75-77] shows that the central region of our Galaxy in general, and the central supermassive Black Hole Sgr A\* in particular, could significantly contribute to the hadronic component of galactic cosmic rays up to  $10^{15}$  eV, and perhaps even to  $10^{18}$  eV [78, 79] although, of course, the electronic origin of the detected TeV radiation remains a possible alternative [79, 80].

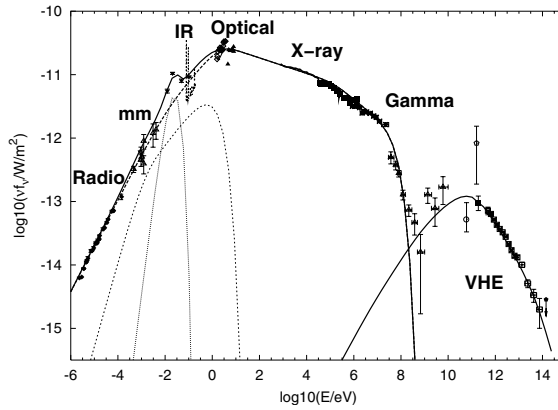


Figure 11: Broad-band SED of the Crab Nebula. The termination shock of the pulsar wind is an extreme accelerator boosting the energy of electrons to  $10^{15}$  eV and beyond. In the framework of the synchrotron/inverse Compton emission model, it is possible to explain the entire energy range from radio wavelengths to ultra-high energy gamma-rays. While the synchrotron radiation of  $\geq 10^{14}$  eV electrons extends to the multi-MeV region, the inverse Compton scattering of the same electrons results in the ultra-high energy gamma-radiation detected by the HEGRA IACT system up to 50 TeV and beyond (see for details [71]).

## 9. SEARCHING FOR COSMIC ACCELERATORS WITH GLAST AND IACT ARRAYS

The main obstacle to revealing the production sites and acceleration mechanisms of CRs is the effective diffusion of charged particles in interstellar magnetic fields, which results in confusion of individual contributors to the “sea” of galactic CRs, and significantly modifies the original (source) spectra of accelerated particles. Therefore, it is believed that the resolution of these long-standing questions will be provided by gamma-ray astronomy, i.e. through *indirect* but (almost) model-independent measurements of secondary  $\gamma$ -rays. The recent exiting discoveries of TeV gamma-radiation from several galactic source populations, in particular from shell-type SNRs, with the HESS array of imaging atmospheric Cherenkov telescopes fully

confirm the early expectations.

Generally the atmospheric Cherenkov telescopes are designed for detection of  $\gamma$ -rays from point like sources. However, the (relatively) large field of view of the HESS telescopes and the stereoscopic approach of reconstruction of air shower parameters allow adequate studies of reasonably extended (up to  $2^\circ$ ) sources, as well as effective surveys of limited regions of the sky. The Galactic Disk is obviously the highest priority target for such a survey. This allows not only search for new type of yet unknown TeV emitters, but also effective study of diffuse galactic  $\gamma$ -ray emission on *small* ( $\leq 100$  pc around the cosmic accelerators) and *large* (kpc) scales. Note that although generally the kpc scale diffuse galactic  $\gamma$ -ray emission is treated as a truly diffuse radiation component caused by interactions of the "sea" of galactic CR ray electrons and protons with the ambient gas and photon fields (see e.g. Ref.[81]), the contribution of discrete sources, e.g. old SNRs [82] can be quite significant.

The spectra of particle acceleration (e.g. by SNR shocks) are generally expected to be significantly harder than the locally observed spectrum of CRs. On the other hand, the confinement time of particles in the source decreases with energy (the leakage of particles becomes easier at higher energies), therefore the quasi-stationary spectrum of particles established in the source could be significantly steeper than the acceleration spectrum. Correspondingly, even for a hard, e.g.  $E^{-2}$  type, particle acceleration spectrum, the secondary  $\gamma$ -rays produced by interactions of relativistic particles inside the sources, could have quite a steep spectrum – just opposite to the common belief in which the hardest  $\gamma$ -ray spectra are expected from CR accelerators themselves.

This effect is illustrated in Fig. 12. It is assumed that high energy protons are injected into a dense region of size  $R = 3$  pc, gas density  $n = 100 \text{ cm}^{-3}$ , and magnetic field  $B = 100 \mu\text{G}$ . These parameters are typical for the so-called giant molecular clouds – possible sites of particle acceleration and gamma-ray production. The acceleration spectrum of protons is assumed to be a power-law with an index  $\alpha = 2.1$ , and exponential cutoff at  $10^{15} \text{ eV}$ . The time history of acceleration is assumed as  $L = L_0(1 + t/\tau_0)^{-2}$ , with  $L_0 = 10^{38} \text{ erg/s}$  and  $\tau_0 = 10^3 \text{ yr}$ . This assumption implies that the acceleration rate was essentially constant over the first  $10^3$  years, but has later decreased with time as  $t^{-2}$ . Finally, the confinement time of particles was approximated in the form  $t_{\text{esc}} = R^2/2D(E) \approx 4 \times 10^4 \kappa^{-1} (E/100 \text{ TeV})^{-1} \text{ yr}$ , where  $\kappa = 1$  corresponds to the slowest possible escape in the Bohm diffusion regime. One can see that for the chosen parameters of the ambient medium and acceleration rate, the proton escape results in a significant suppression of TeV  $\gamma$ -rays, especially at observation epochs  $t \geq 10^4 \text{ yr}$ , even if the particle escape proceeds in the regime close to the Bohm diffusion.

Thus, the study of a cosmic accelerator by detecting  $\gamma$ -rays from the central source cannot be complete because it contains information only about relatively low-energy particles effectively confined in the source. In many cases the detection of  $\gamma$ -rays from regions surrounding the accelerator could add much to our knowledge about the highest energy particles which quickly escape from the source and thus do not con-

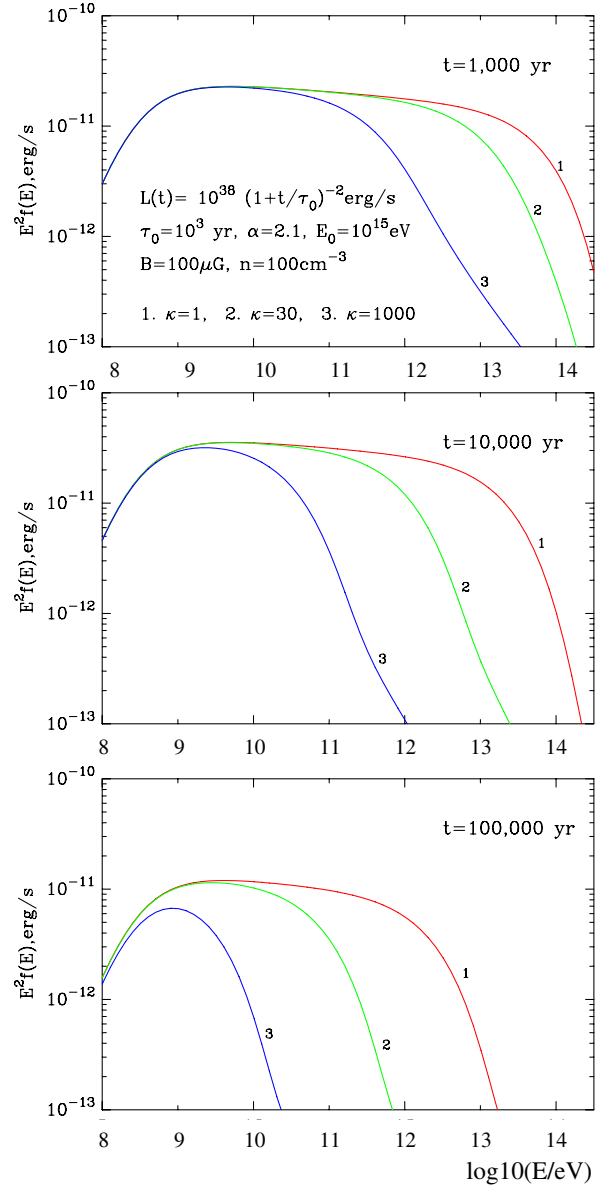


Figure 12: Expected  $\gamma$ -ray spectra at different observation epochs –  $t = 10^3, 10^4$  and  $10^5$  years after the start of operation of the proton accelerator, for three different assumptions concerning the escape time of particles from the  $\gamma$ -ray production region:  $\kappa = 1, 30, 1000$ .

tribute to the  $\gamma$ -ray production inside the source.

For “typical” CR accelerators, e.g. SNRs with a total energy release in protons of less than  $W \leq 10^{50}$  erg, the extension of these regions cannot significantly exceed several tens of parsecs, because at such large distances from the source, the density of relativistic particles becomes negligible compared to the level of the “sea” of galactic CRs.

The existence of a powerful particle *accelerator* by itself is not yet sufficient for effective  $\gamma$ -ray production. Clearly, an additional component – a dense gas target – is required. Giant Molecular Clouds (GMCs) are perfect objects to play that role in our Galaxy. They are physically connected with star formation regions which are believed to be the most probable sites for the production of galactic cosmic rays. Fig. 13 illustrates [83] the  $\gamma$ -ray production by a cloud located in the vicinity of a particle accelerator where the energy density of CRs can significantly exceed the level of the “sea” of galactic CRs of about  $1 \text{ eV/cm}^3$ . It is possible that the two unidentified TeV sources discovered by HEGRA telescope system [84] and by HESS [85] belong to this class of objects.

The remarkable feature of  $\gamma$ -radiation of GMCs is the strong evolution in time of both the absolute fluxes and the spectra of  $\gamma$ -rays. The character of the evolution essentially depends on the diffusion coefficient  $D(E)$  and distance  $R$  between the target and accelerator. Depending on the combination of the diffusion coefficient  $D(E)$ , distance  $R$ , as well as the age of the accelerator  $t$ , one should expect quite different  $\gamma$ -ray spectra from source to source. Namely, in the case of a cloud near a relatively young accelerator the differential  $\gamma$ -ray spectrum is expected to be much harder than the primary spectrum of the accelerated particles, i.e.  $\Gamma < 2$ . Meanwhile, the  $\gamma$ -ray spectra from clouds located near old accelerators would be soft, with a spectral index  $\Gamma \geq 2.7$ .

Thus, the detection of  $\gamma$ -rays from different clouds located at different distances from the accelerator may provide unique information about the diffusion coefficient  $D(E)$  as well as about the age of the accelerator. Similar information may be obtained detecting  $\gamma$ -rays from the same cloud, but in different energy domains, namely at GeV and TeV energies.

It should be noted that in the case of energy-dependent propagation of cosmic rays the chance of simultaneous detection of a cloud in GeV and TeV  $\gamma$ -rays could be not very high, because the maximum fluxes at these energies are reached at different epochs. Since the higher energy particles propagate faster and therefore reach the cloud earlier, the maximum of GeV  $\gamma$ -radiation appears at an epoch when the maximum of the TeV  $\gamma$ -ray flux has already passed. In the case of energy-independent propagation (e.g. due to strong convection) the ratio of fluxes  $F_\gamma(\geq 100 \text{ MeV})/F_\gamma(\geq 1 \text{ TeV})$  is independent of time, therefore the clouds which are visible at GeV energies

would be detectable also at TeV energies.

In Fig. 13 are shown the temporal evolution of the integral  $\gamma$ -ray fluxes in the energy intervals between 0.3-3 GeV and 1-10 TeV from a cloud with  $M_5/d_{\text{kpc}}^2 = 1$  (where  $M_5 = M/10^5 M_\odot$  is the mass of the cloud in units of  $10^5$  solar masses, and  $d_{\text{kpc}} = d/1\text{kpc}$  is the distance to the source in units of kpc), located at 10 pc, 30 pc, and 100 pc distances from an *impulsive* proton accelerator with  $W_p = 10^{50}$  erg. For the diffusion coefficient is assumed  $D_* = 10^{27}(E/1\text{GeV})^{0.5} \text{ cm}^2/\text{s}$ , which implies an order of magnitude slower diffusion

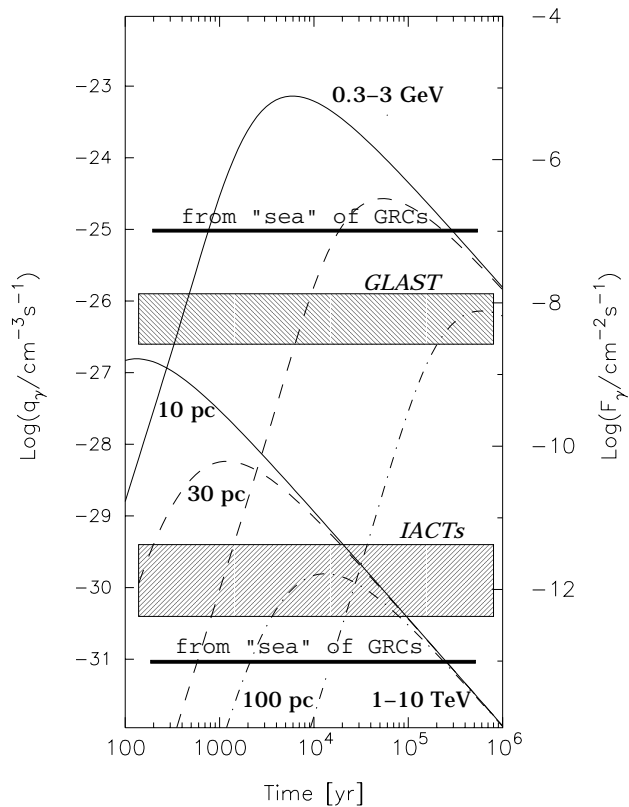


Figure 13: Time dependence of the  $\pi^0$ -decay  $\gamma$ -ray emissivities (the left-hand side ordinate axes) and the fluxes (the right-hand side ordinate axes) from a cloud in the energy intervals 0.3-3 GeV and 1-10 TeV at three different distances from an *impulsive* accelerator: 10 pc, 30 pc, and 100 pc. The fluxes are calculated for a GMC with  $M_5/d_{\text{kpc}}^2 = 1$  and a proton accelerator with  $W_p = 10^{50}$  erg. The horizontal lines indicate the corresponding emissivities and fluxes of  $\gamma$ -rays expected from the “sea” of galactic CRs. The expected sensitivities of GLAST and the next generation of IACT arrays in the same energy intervals are shown for the range of the  $\gamma$ -ray source size between  $0.1^\circ$  and  $1^\circ$  (see Ref. [83] for details).

than in the standard parts of the Galactic Disk.

The comparison of the expected  $\gamma$ -ray fluxes with the sensitivities of GLAST (for approximately 1 year observation time), and IACT arrays like HESS (for  $\approx 10$  h of observation time), show that at certain (not necessarily same) epochs the cloud could be visible at GeV and/or TeV energies, up to distances to the accelerator  $R \sim 30$  pc even for the source size of about  $1^\circ$ , provided that  $W_{50} M_5 d_{\text{kpc}}^{-2} \geq 0.01$ .

The  $\gamma$ -ray emission outside cosmic accelerators contains unique information not available in the case of direct observations of the accelerators themselves. This allows not only correct estimates of the total energy budget of the accelerator, but also reconstruction of the time history of the accelerator, the maximum energy of accelerated particles, etc. In particular, the detection of possible spectral cutoffs in the  $\gamma$ -ray spectra of SNRs at  $E \leq 10$  TeV cannot be unambiguously related to the inability of the source to accelerate particles to energies 100 TeV or beyond. This could be rather connected with the escape of most energetic particles which were accelerated at the early stages of the SNR but at the present epoch (of observations) already have left the source (see e.g. Refs.[86]). Therefore the secondary products of these particles - the  $\pi^0$ -decay  $\gamma$ -rays would have more chances to be detected outside of the source rather than from the source. On the other hand, the chances to detect  $\gamma$ -rays from old SNRs is higher at GeV, rather than at TeV energies.

In this regard, GLAST and the stereoscopic IACT arrays are complementary instruments, and the study of cosmic ray accelerators in our Galaxy can be conducted most effectively through coordinated observations by GLAST and HESS type telescope arrays located both in Northern and Southern hemispheres.

## 9.1. Acknowledgments

I thank the members of the HESS and HEGRA collaborations, as well as Y. Uchiyama and V. Zirakashvili for many helpful discussions. I am grateful to the organizers of the XXII Texas Symposium on Relativistic Astrophysics for inviting me to give this plenary talk.

## References

- [1] P. Morrison 1957, Nuovo Cimento **7**, 858.
- [2] V.L. Ginzburg, S.I. Syrovatskii, "Origin of Cosmic Rays", Macmillan, 1963.
- [3] T.K. Gaisser, Proc. 31st Intern. Conf. on High Energy Physics, Amsterdam, July 2002.
- [4] F. Halzen 2005, in Proc. 2nd Intern. Symposium on High Energy Gamma Ray Astronomy, AIP Conf. Proc. **745**, Melville, NY, p.3.
- [5] V.S. Berezinsky, S.V. Bulanov, V.L. Ginzburg, V.A. Dogiel V.A. and V.S. Ptuskin, "Astrophysics of Cosmic Rays", North-Holland, 1990.
- [6] F.A. Aharonian 2001, Space Sci. Rev. **99**, 187.
- [7] A.D. Erlykin, A.W. Wolfendale 2005, Astropart. Phys. **23**, 1.
- [8] S.D. Hunter, D.L. Bertsch, J.R. Catelli et al. 1997, ApJ **481**, 205.
- [9] J. Nishimura et al. 1980, ApJ **238**, 394.
- [10] F.A. Aharonian, A.M. Atoyan, A.M., H.J. Völk 1995, A&A **294**, L41.
- [11] T. Kobayashi, Y. Komori, K. Yoshida, J. Nishimura, J. 2004, ApJ **601**, 340.
- [12] A.W. Wolfendale, "The Hess Memorial Lecture", in Proc. 23rd ICRC (Calgary), *Invited, Rappoiteur & Highlight papers*, World Scientific, p. 143.
- [13] M.A. Malkov, L.O'C. Drury 2001, Rep. Prog. Phys. **64**, 429.
- [14] M.A. Malkov 1997, ApJ **485**, 638.
- [15] E.G. Berezhko, D.C. Ellison 1999, ApJ **526**, 385.
- [16] P. Blasi, S. Gabici, G. Vannoni 2005, MNRAS, submitted.
- [17] L.O'C. Drury, F:A: Aharonian, H.J. Volk A&A **287**, 959.
- [18] T. Tanimori et al (CANGAROO collaboration) 1998, ApJ **497**, L25.
- [19] F.A. Aharonian (HEGRA Collaboration) 2001, A&A **370**, 112.
- [20] H. Muraishi et al. (CANGAROO Collaboration) 2000, A&A **354**, L57.
- [21] J.H. Buckley, A.C. Akerlof, C.W. Carter-Lewis et al. (Whipple Collaboration) (1998), A&A **329**, 639.
- [22] F.A. Aharonian, W. Hofmann, A. Konopelko, H.J. Völk 1997, Astropart. Phys. **6**, 343; 369.
- [23] F.A Aharonian, C. Akerlof 1997, Ann. Rev. Nucl. Part Sci. **47**, 273.
- [24] R. Ong 1998, Physics Reports **305**, 93.
- [25] M. Catanese, T.C. Weekes 1999, PASP **111**, 1193.
- [26] C.M. Hoffman, C. Sinnis, C., P. Fleury, M. Punch 1999, Reviews of Modern Physics **71**, 897.
- [27] K. Bernlöhr, O. Carol, R. Cornelis et al. 2003, Astropart. Phys. **20**, 111.
- [28] P. Vicent, J.-P. Denance, J.F. Huppert et al. 2003, in Proc 28th ICRC, Tsukuba (Univ. Academy PressHESSperformance), 2887.
- [29] W. Benbow et al. (HESS collaboration) 2005, in Proc. 2nd Intern. Symposium on High Energy Gamma Ray Astronomy, AIP Conf. Proc. **745**, Melville, NY, p. 611.
- [30] F.A. Aharonian et al. (HESS collaboration) 2004, Nature **432**, 75.
- [31] F.A. Aharonian et al. (HESS collaboration) 2005a, A&A, submitted.
- [32] F. Pfeffermann, B. Aschenbach 1997, in Röntgensstrahlung from the Universe, MPE Report 263, Garching, 267.

- [33] K. Koyama et al. 1997, PASJ **49**, L7.
- [34] P. Slane et al. 1999, ApJ **525**, 357.
- [35] Y. Uchiyama, T. Takahashi, F.A. Aharonian 2002, PASJ **54**, L73.
- [36] Y. Uchiyama, F.A. Aharonian, T. Takahashi 2003, A&A **400**, 567.
- [37] G. Cassam-Chenai, A. Decourchelle, J. Ballet et al. 2004, A&A **427**, 199.
- [38] J.S. Hiraga, Y.Uchiyama, T. Takahashi, F.A. Aharonian 2005, A&A **431**, 953.
- [39] R. Enomoto et al. (CANGAROO Collaboration) 2002, Nature **416**, 823.
- [40] F. A. Aharonian et al. (HESS Collaboration) 2004, Nature **432**, 75.
- [41] F. A. Aharonian et al. (HESS Collaboration) 2005, in preparation.
- [42] Y. Fukui et al. 2003, PASJ **55**, L61.
- [43] Z.R. Wang, Q.-Y. Qu, Y. Chen 1997, A&A **318**, L53.
- [44] H. Katagiri et al. (CANGAROO Collaboration) 2005, ApJ **619**, L163.
- [45] F.A. Aharonian et al. (HESS Collaboration) 2005, A&A, submitted.
- [46] B. Aschenbach 1998, Nature **396**, 141.
- [47] B. Aschenbach, A.F. Iyudin, V. Schönfelder 1999, A&A **350**, 997.
- [48] P. Slane et al. 2001, ApJ **548**, 814.
- [49] T. Tanimori et al. (CANGAROO Collaboration) 1998 ApJ **497**, L25.
- [50] A. Mastichiadis, O.C. De Jager 1996, A&A **311**, L5.
- [51] T. Yoshida, S. Yanagita 1997, in Proc 2nd INTEGRAL Workshop on the Trtansparent Universe, SP-382, ESA, Paris, p.85.
- [52] F.A. Aharonian, A.M. Atoyan 1999, A&A **351**, 330.
- [53] Baring, M.G., Ellison, D.C., Reynolds, S.P., Grenier,I.A. and Goret, P. (1999) ApJ **513**, 311.
- [54] E.G. Berezhko, L.T. Ksenofontov, H.J. Völk 2002, A&A **395**, 943.
- [55] F.A. Aharonian et all. (HESS collaboration) 2005, A&A, in press.
- [56] R. Cowsik, S.Sarkar 1980, MNRAS **191**, 855.
- [57] A.M. Atoyan, F.A.Aharonian, R.Tuffs, H.J. Völk 2000, A&A **355**, 211.
- [58] J. Vink 2005, in Proc. 2nd Intern. Symposium on High Energy Gamma Ray Astronomy, AIP Conf. Proc. **745**, Melville, NY, p. 160.
- [59] E.G. Berezhko, G. Phlhofer, H.J. Völk 2003, A&A **400**, 971.
- [60] J.R. Jokipii 1987, ApJ **313**, 842.
- [61] O. Reimer, M. Pohl 2002, A&A **390**, L43.
- [62] Y.M. Butt et al. 2002, Nature **418**, 499.
- [63] F.A. Aharonian 2001, Space Sci. Rev. **99**, 187.
- [64] M.A. Malkov, P.H. Diamond, R.Z. Sagdeev 2005, ApJ Letters, in press.
- [65] R.M. Crutcher 1999, ApJ **520**, 706.
- [66] J. S. Lazendic et al. 2004, ApJ **602**, 271.
- [67] A. Bykov et al. 2000, ApJ **538**, 203
- [68] F.A. Aharonian et al. (HESS collaboration) 2005a, A&A **432**, L25
- [69] F.A. Aharonian et al. (HESS collaboration) 2005b, A&A, submitted
- [70] F.A. Aharonian et al. (HESS collaboration) 2005c, A&A, submitted
- [71] F.A. Aharonian et al. (HEGRA collaboration) 2005, ApJ **614**, 897
- [72] J. Arons 1996, Space Sci. Rev. **75**, 235.
- [73] E. Amato, D. Guetta, D., P. Blasi 2003, A&A **402**, 827.
- [74] W. Bednarek 2003, A&A **407**, 1.
- [75] K. Tsuchiya et al. (CANGAROO collaboration) 2004, ApJ **606**, L115.
- [76] K. Kosack et al (Whipple collaboration) 2004, ApJ **608**, L97.
- [77] F.A. Aharonian et al. (HESS collaboration) 2004, A&A **425**, L13
- [78] R. Crocker, F. Melia, R. Volkas 2005, ApJ **622**, L37.
- [79] F.A. Aharonian, A. Neronov 2005, ApJ **619**, 306.
- [80] A. Atoyan, C. Dermer 2004, ApJ **617**, L123.
- [81] A.W.Strong, I.V. Moskalenko, O. Reimer 2004, ApJ **613**, 962.
- [82] E.G. Berezhko, H.J. Völk 2004, ApJ **611**, 12.
- [83] F.A. Aharonian 1995, Nucl. Phys. B **39A**, 193.
- [84] F.A. Aharonian (HEGRA collaboration) 2005, A&A **431**, 197.
- [85] F.A. Aharonian (HEGRA collaboration) 2005, A&A, submitted.
- [86] V.S. Ptuskin, V.N. Zirakashvili 2005, A&A **429**, 755.